

## **P1.6 HIGH RESOLUTION ASSIMILATION OF CASA RADAR DATA FROM A TORNADIC CONVECTIVE SYSTEM**

Alexander D. Schenkman\*, Alan Shapiro, Keith Brewster, Ming Xue, Jidong Gao, and Nathan Snook, University of Oklahoma, Norman, OK

### **1. INTRODUCTION**

In late 2006, the NSF Engineering Research Center (ERC) for Collaborative and Adaptive Sensing of the Atmosphere (CASA, McLaughlin et al. 2005) began its first integrated project (IP1, Brotzge et al. 2007). CASA-IP1 consists of a network of four x-band dual-polarization Doppler radars in southwest Oklahoma.

During the spring of 2007, this radar network collected data from a number of severe convective events. As part of the CASA spring Experiment 2007 (CSET-2007, Brewster et al. 2007), quasi real-time forecasts were performed using the CAPS ADAS analysis system (Brewster 1996). Preliminary results from these "real-time" forecasts showed success from assimilating combined reflectivity from WSR-88D and CASA radars.

This paper is concerned with the assimilation of CASA radar data into the three-dimensional variational data assimilation (3DVAR) package of a non-hydrostatic numerical model, the Advanced Regional Prediction System (ARPS). The ARPS 3DVAR minimizes a cost function that includes the departure of the analysis from the background, the departure of the observations from the analysis and a penalty term. The penalty term imposes a weak anelastic mass continuity constraint on the analyzed wind field. The ARPS 3DVAR is described in detail in Gao et al. 2004 and Hu et al 2006b.

Previous work found that 3DVAR reflectivity assimilation is most effective when combined with a cloud analysis (Hu et al. 2006a, Hu et al. 2006b). By expediting the "spin-up" of important convective cells and associated clouds, a cloud analysis improves the accuracy of the overall analysis (Hu et al. 2006a, Hu and Xue 2007). The cloud analysis used in this study evolved from the Local Analysis and Prediction System (LAPS, Albers et al. 1996) with modifications by Zhang (1998) and Brewster (2002).

In this study, we use 3DVAR and a cloud analysis to analyze a mesoscale convective vortex (MCV; e.g. Johnston 1981; Menard and Fritsch 1989) that developed and moved through southwest and central Oklahoma on 8-9 May 2007. This MCV was observed by the WSR-88D KTLX and KFDR as well as all four CASA radars during CSET-2007. The ARPS is used to assimilate radar data and forecast the evolution of the MCV. The impact of assimilating radial velocity and reflectivity from CASA in addition to WSR-88D data is examined. We hypothesize that the assimilation of CASA data will mainly affect high resolution experiments as these experiments can take advantage of the high spatial resolution of CASA data.

This paper is organized as follows: In section 2, the 8-9 May 2007 southwest/central Oklahoma MCV case is described. Model parameters, experiment configurations and data are presented in section 3. In section 4, experiment results are described and compared to actual observations. In section 5, we present preliminary conclusions and an outline of the future of this ongoing work.

### **2. EVENT DISCUSSION**

On the morning of 8 May 2007, a large complex of thunderstorms developed in far eastern portions of New Mexico in an area of upslope flow and moisture advection. A short wave trough ejecting from a large trough in the southwestern US likely aided in this thunderstorm development. The thunderstorm complex grew in areal extent and was located from southwest Oklahoma south to near Del Rio, TX at 0000 UTC 9 May 2007. The Texas portion of the complex began to dissipate shortly after 0000 UTC while new supercell-like development in southwest Oklahoma allowed the line to persist until around 0700 UTC.

Around 22:00 UTC an MCV developed in the northern portion of the thunderstorm complex in the vicinity of Wichita Falls, TX. This MCV strengthened and contracted while moving north-northeast into southwest Oklahoma. A supercell in Comanche county Oklahoma was absorbed by

---

\* *Corresponding author address:* Alexander D. Schenkman, Univ. of Oklahoma, School of Meteorology, Norman, OK 73072; e-mail: alex3238@ou.edu.

the MCV leading to a rapid intensification of the MCV circulation evident in both radar and Oklahoma Mesonet 10m wind observations. Even as the majority of the thunderstorm complex weakened, the MCV continued to strengthen as it moved through Grady and Canadian counties with the first confirmed tornado occurring near Minco at 0354 UTC (Fig. 1a). Another confirmed tornado produced strong EF-1 damage in El Reno, OK around 04:45 UTC (Fig. 1b). The MCV weakened after 0500 UTC and eventually dissipated around 0800 UTC.

### 3. METHODOLOGY

#### 3.1 Model configuration

The non-hydrostatic ARPS model was used in this study. Lin et al. 1983 ice microphysics were used with a modified rain intercept parameter of  $8.0 \times 10^5$ . This rain intercept value was used because it is more representative of convective rain than the value used in that study.

#### 3.2 Grid configuration

Experiments are conducted on two (nested) grids. A relatively coarse outer grid, with 2 km horizontal resolution, is used to initialize an inner grid with a fine horizontal grid spacing of 400 m. The outer grid is 1000km x 1000km, while the inner grid is a 120km x 120km subsection of the outer grid (Fig. 2).

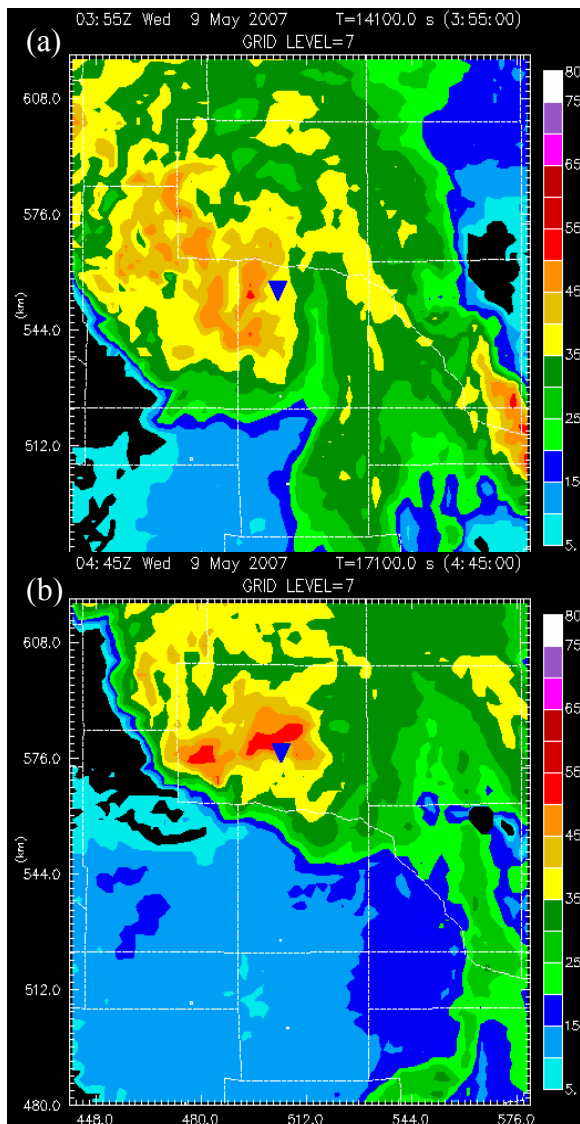


Fig. 1. Reflectivity factor from KTLX from (a) 0355 UTC 9 May 2007 and (b) 0445 9 May 2007. Blue triangles are confirmed tornado locations from National Weather Service storm reports.

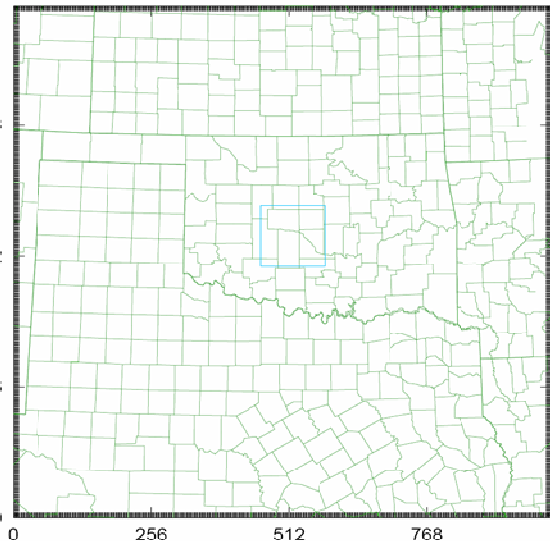


Fig. 2. Map of the outer grid. The blue square is the inner domain.

The 0000 UTC 12km resolution version of the National Center for Environmental Prediction's (NCEP) North American Model (NAM) was used to provide a background and boundary conditions to the outer nest. The inner grid is initialized using model output from the outer grid. The nesting is one-way, i.e. fields on the inner grid do not impact the outer grid. Both model grids use stretched grid spacing in the vertical with minimum spacing of 100m. There are 43 vertical levels for the outer nest, and 63 vertical levels for the inner nest.

### 3.3. Data

A wide range of data sources were used in the 3DVAR analyses. The ARPS 3DVAR analysis package allows for different sources of data to be analyzed during separate analysis passes, with user specified horizontal and vertical influence radii. Because of their different spatial resolution, the two grids used different values for the influence radii. In this way, data assimilation on the high resolution grid is able to take advantage of the high spatial resolution of CASA data. The filter scale for first, second and third analysis passes on the outer grid were 200 km, 75 km and 4 km respectively. The inner grid used 20 km, 5 km, and 0.8 km for its analysis passes.

Upper air data as well as profiler data are used on the first analysis pass. These data have the coarsest spatial resolution and thus the first pass is used to analyze them because it has the largest influence radius. Hourly data from ASOS stations, the Oklahoma Mesonet (Brock et al. 1995), and aircraft observations (MDCRS) are analyzed on the second analysis pass.

Level – II radar data from WSR-88D and CASA are utilized during the third analysis pass. On the outer grid, data from six WSR-88Ds are used: KTLX, KVNK, KFWS, KAMA, KDYX, and KLBB. The inner grid uses data from KTLX and KVNK only. The WSR-88D in southwest Oklahoma, KFDR, was not used because level-II data were not available from the National Climatic Data Center's (NCDC) Robotic Mass Storage System. In experiments utilizing CASA data, the inner and outer grids use data from all four CASA radars.

Pre-processing is performed to map radar data from radar coordinates onto a Cartesian grid. Additionally, radar data are despeckled and dealiased. Details of this pre-processing can be found in Brewster et al 2005b.

It must be noted that the pre-processing routine assumes data are available in the format of WSR-88D volumetric radar data. This is somewhat problematic for CASA radar data, as the CASA radars perform sector scans. However, each CASA radar scans at least one (at most three) full 360° each minute (typically, at the lowest elevation angle). Thus radar pre-processing takes the 360° scan in combination with 4-6 sector scans and builds a pseudo-volume. Areas that are not scanned are left as missing data and are not used in the analysis.

### 3.4. Analysis cycles

An initial analysis is performed at 0000 UTC using conventional data (RAOBS, SAO, OK Mesonet) and the NAM as a background. A one hour forecast is then run to allow for “spin-up” of key features. The results of this one hour forecast are used as the background for experiments utilizing radar. The conventional observation experiment is also run out to 0500 UTC for comparison purposes.

Experiments that utilize radar data are conducted with a one hour time window (01-02 UTC) of five minute assimilation cycles (Fig 3). Upon performing the 0200 UTC analysis the model is run to 0500 UTC. A cloud analysis (described in section 1) is also performed during each analysis. However, qc and qv are only adjusted during the 0100Z analysis after preliminary tests showed that adjustments at multiple times would put too much moisture into the model.

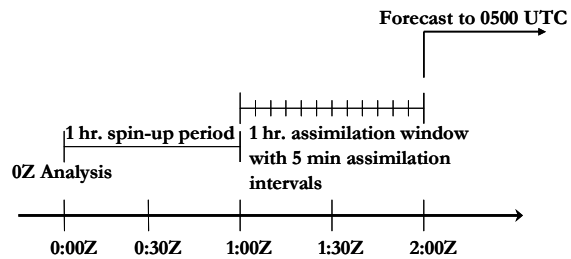


Fig 3. Schematic of the assimilation window.

### 3.5 Experiment configurations

Nine experiments were performed to examine the impact of assimilating CASA radar data. With the exception of the control run (EXP0), which assimilated no radar data, all experiments used radial velocity ( $V_r$ ) and reflectivity ( $Z$ ) from the WSR-88D. In the experiments with assimilated radar data, one was run without CASA, one had both  $V_r$  and  $Z$  from CASA, another used only CASA  $V_r$ , and a final experiment used just  $Z$  from CASA. Table 1 summarizes the experiments.

Experiment	CASA	88D	Resolution
EXP0	None	None	2km
EXP1	None	$V_r$ and $Z$	2km
EXP2	$V_r$ and $Z$	$V_r$ and $Z$	2km
EXP3	$V_r$	$V_r$ and $Z$	2km
EXP4	$Z$	$V_r$ and $Z$	2km
EXP5	None	$V_r$ and $Z$	400m
EXP6	$V_r$ and $Z$	$V_r$ and $Z$	400m
EXP7	$V_r$	$V_r$ and $Z$	400m
EXP8	$Z$	$V_r$ and $Z$	400m

Table 1. Experiments and their characteristics.

## 4. EXPERIMENT RESULTS

A general description of the outcome of the experiments is presented in this section. For the sake of brevity, results are primarily described with a focus on two times: the 0354 UTC Minco tornado and the 0445 UTC El Reno tornado. Additionally, descriptions of model runs with assimilated radar data will focus on differences between the outcomes of experiments.

### 4.1. Control experiment

A small area of convection is present in southwest Oklahoma at the beginning (0200 UTC) of the control run (not shown). This convection is not well organized and consists of a few thunderstorms without any apparent circulation. With time convection becomes better organized and several small vorticity centers are embedded within the stronger convective cells. A MCV does not form. Outside of convective cells, winds are uniform from the southeast.

At 0355 UTC a stronger vorticity center develops in the southeast Grady county (Fig. 4a). This vorticity center moves northeast and slowly weakens. By 0445 UTC the main body of the complex has moved to an arc from northern Canadian to Oklahoma to Cleveland and McClain counties (Fig. 4b). A weak surface low is present (not shown), however, there is no MCV type organization.

### 4.2. 2km resolution experiments

#### 4.2.1 Experiment without CASA data

In EXP1, a large MCS is present over Oklahoma and western-north Texas at 0200 UTC. The portion of the MCS in Texas rapidly weakens and only scattered convection remains by 0230 UTC. Meanwhile, the Oklahoma portion of the MCS maintains a line of convection that becomes well organized. A MCV is clearly evident by 0300 UTC.

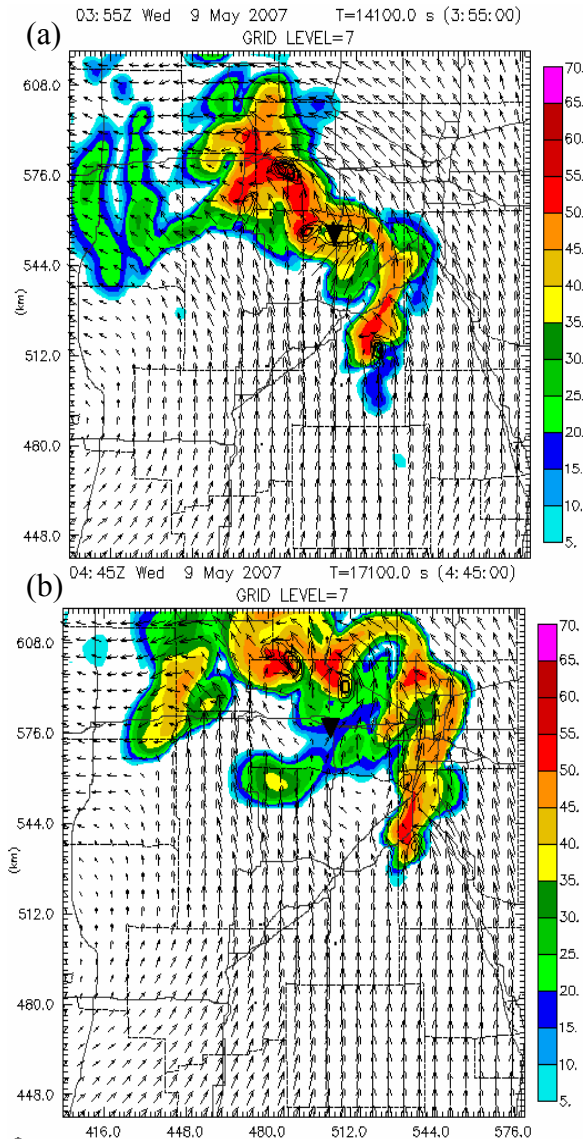


Fig. 4. Forecast at grid level 7 ( $z \sim 1.5\text{km}$ ) from EXP0 at (a) 0355 UTC and (b) 0445 9 May 2007. Reflectivity is shaded, contours are vorticity, and the black triangle indicates the reported tornado location.

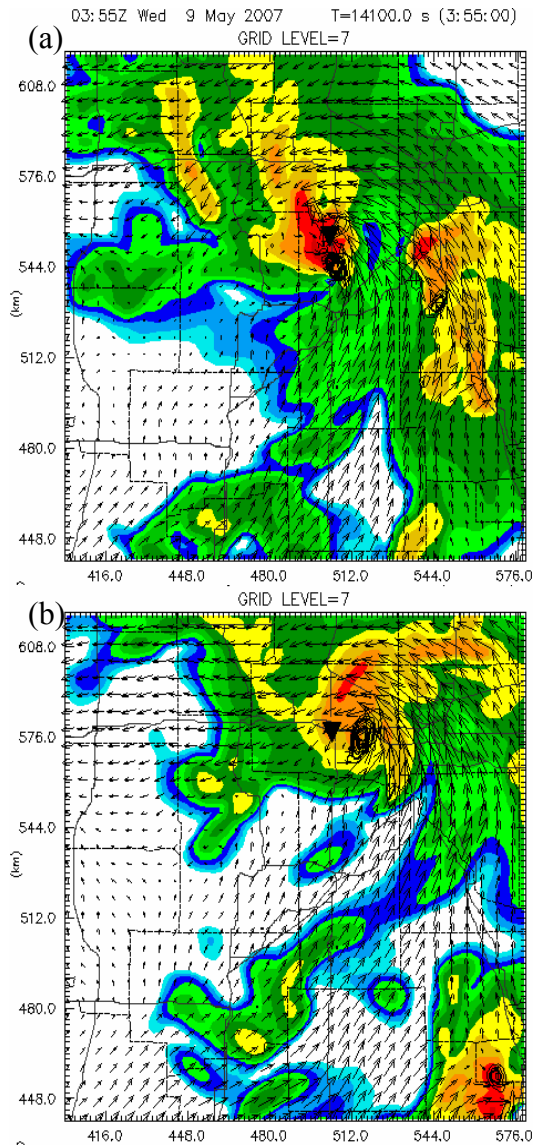


Fig. 5 As Fig. 4 but for EXP1.

At 0330 UTC a convective cell develops near the center of the MCV. This cell rapidly strengthens and by 0355 UTC a strong circulation has developed in north central Grady county about 12km south-southeast of the reported Minco tornado (Fig. 5a). Another cell with a circulation is present to the southeast of the main cell. This secondary cell weakens and dissipates by 0415 UTC. As the main convective cell moves northeast, the circulation associated with it moves northward becoming more embedded in the cell. At 0445 UTC a fairly strong, but steadily weakening, circulation is present in southeast Canadian county around 10km east-southeast of the reported El Reno tornado (Fig 5b).

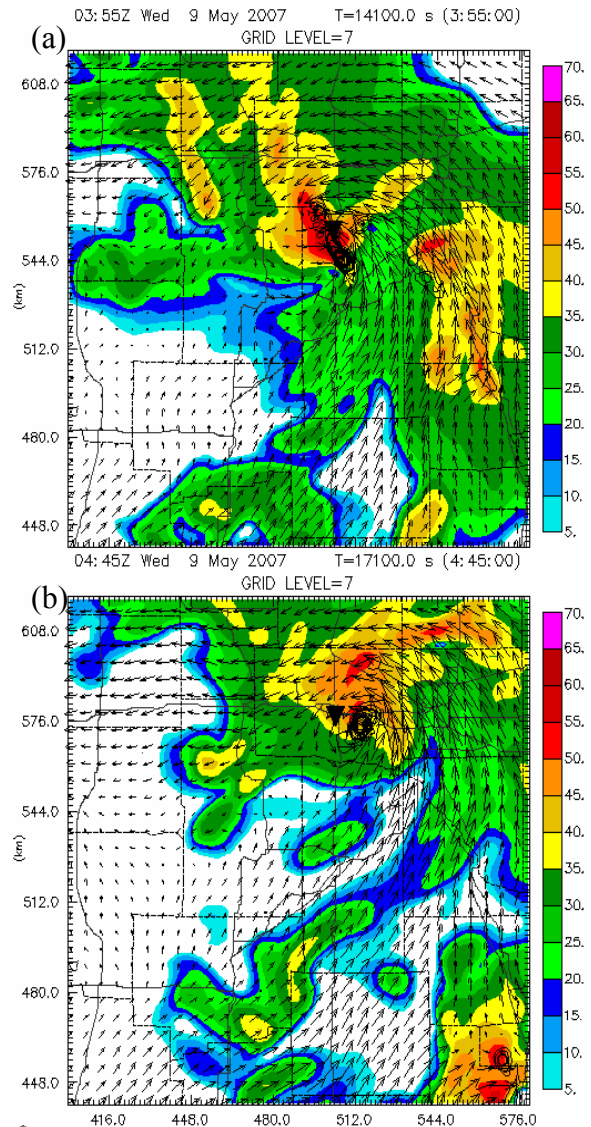


Fig. 6. As Fig. 4 but for EXP2.

#### 4.2.2. Experiments with CASA data

The mesoscale evolution of the MCS and MCV in EXP2 is very similar to EXP1. At the storm scale a few key differences emerge by 0355 UTC. The secondary cell present in EXP1 is much weaker in EXP2 and does not have a circulation. Additionally, the circulation in Grady county is slightly stronger and a bit further northwest (about 12km south-southeast of the reported Minco tornado) than EXP1 (Fig 6a). By 0445 UTC, the main convective cell in EXP2 has a stronger circulation and appears more “wrapped-up” than the cell in EXP1. The circulation is 10 km east-southeast of the reported El Reno tornado (Fig 6b).

EXP3 and EXP4 are very similar to EXP2. One minor difference is that when they are compared to each other. EXP3 develops two vorticity centers around 0400 UTC before merging them around 0425 UTC. EXP4 maintains a single vorticity center throughout the same period (not shown).

### 4.3. 400m resolution experiments

#### 4.3.1 Experiments without CASA data

In EXP5, the MCV enters southwest Oklahoma at 0230 UTC. This line progresses to the northeast with convection near the center of the MCV remaining strong while convection weakens in the tail portion. By 0355 UTC, a fairly strong circulation/ convergence zone develops with the central cell in north-central Grady county about 8 km southeast of the reported Minco tornado (Fig. 7a). The circulation rapidly dissipates as the cell moves to the north-northeast. At 0445 UTC a strong cell is present in Canadian county but no strong consistent low-level circulation is present (Fig. 7b).

#### 4.3.2 Experiments with CASA data

Like the 2km resolution experiments the overall evolution of the MCV with CASA data assimilated (EXP6 - EXP8) is similar to EXP5. However, there are important differences that emerge around 0330 UTC. A strong convective cell develops near the center of the MCV and rapidly develops a low-level circulation. This vortex strengthens rapidly as it moves into north-central Grady county (6 km south of the reported Minco tornado) and by 0355 UTC is more than twice as strong as the circulation from EXP5 (Fig. 8a). Additionally, the vortex is strongest below 2 km, with a maximum vorticity value near  $0.11 \text{ s}^{-1}$ . At 0445 UTC, the convective cell and associated vortex have moved into Canadian county. The vortex has weakened, but is still strong and better defined than EXP5 (Fig. 8b).

Both EXP7 and EXP8 experiments produce stronger vortices at 0355 UTC than EXP5. However, EXP6 has the strongest low-level vortex. EXP8 places the vortex further north in Grady county, closest to the reported tornado (Fig 9a). However, the vortex does not appear as organized as the vortex forecast by EXP7 (Fig 9b).

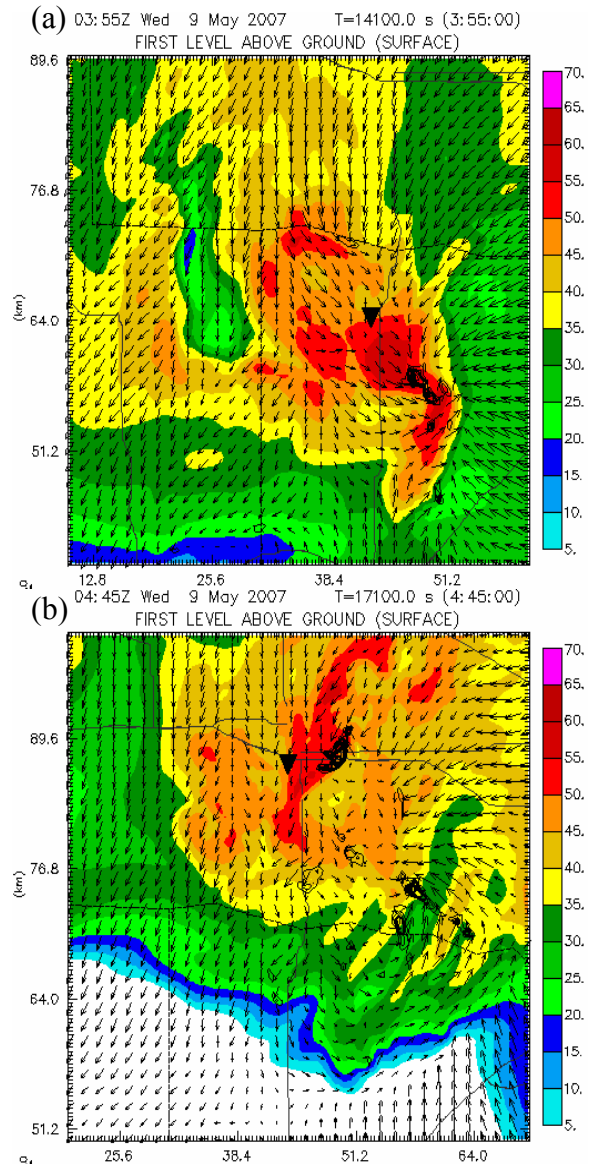


Fig. 7. As Fig. 4 but for EXP5 and at surface level.

## 5. DISCUSSION AND FUTURE WORK

Encouraging results were found from both the 2km and 400m resolution experiments. A subjective comparison with the control experiment shows the assimilation of the radar data in all other experiments leads to large forecast improvements. Additionally, the 2km resolution experiments were able to forecast the development of a strong low-level circulation 115 and 160 min in advance of their formation near Minco and El Reno, respectively. 400 m experiments had great success, especially with CASA data included, forecasting the Minco tornado 115 min in advance.

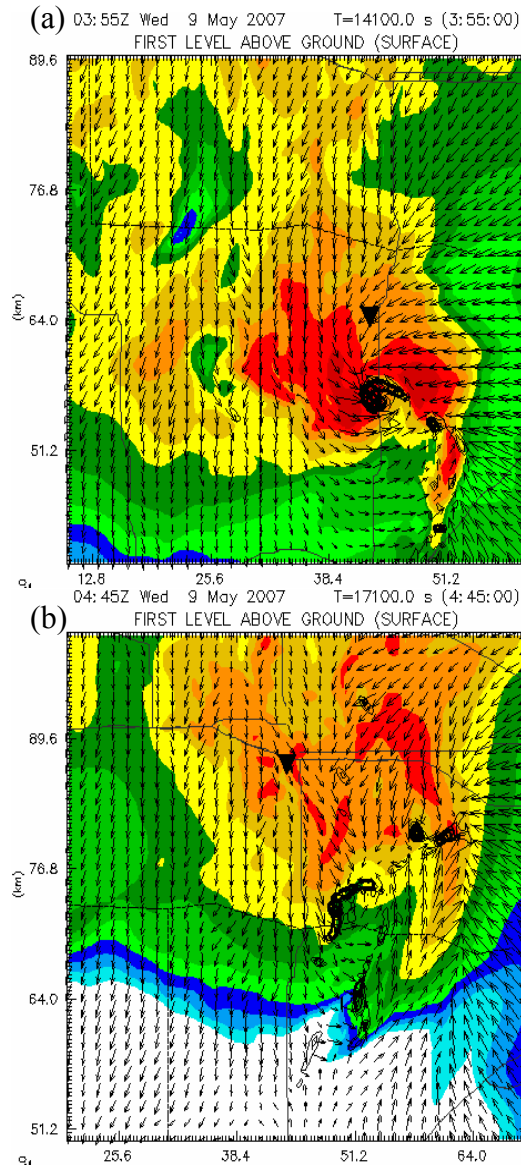


Fig. 8. As Fig. 7 but for EXP6.

The improvement seen from the use of CASA data seems to indicate that the high resolution nature of CASA data can have a large impact on meso and storm scale NWP. Our hypothesis appears to be confirmed as the impacts of CASA data are greatest when assimilated on a high resolution grid. However, to verify this hypothesis future work must be conducted with more test cases and a more objective analysis of results performed, most likely with equitable threat scores (ETS, Schaefer 1990). Additionally, sensitivity experiments that change the assimilation window length as well the grid location must be conducted. Finally, a more detailed look at the output during the analysis window must be performed in order to

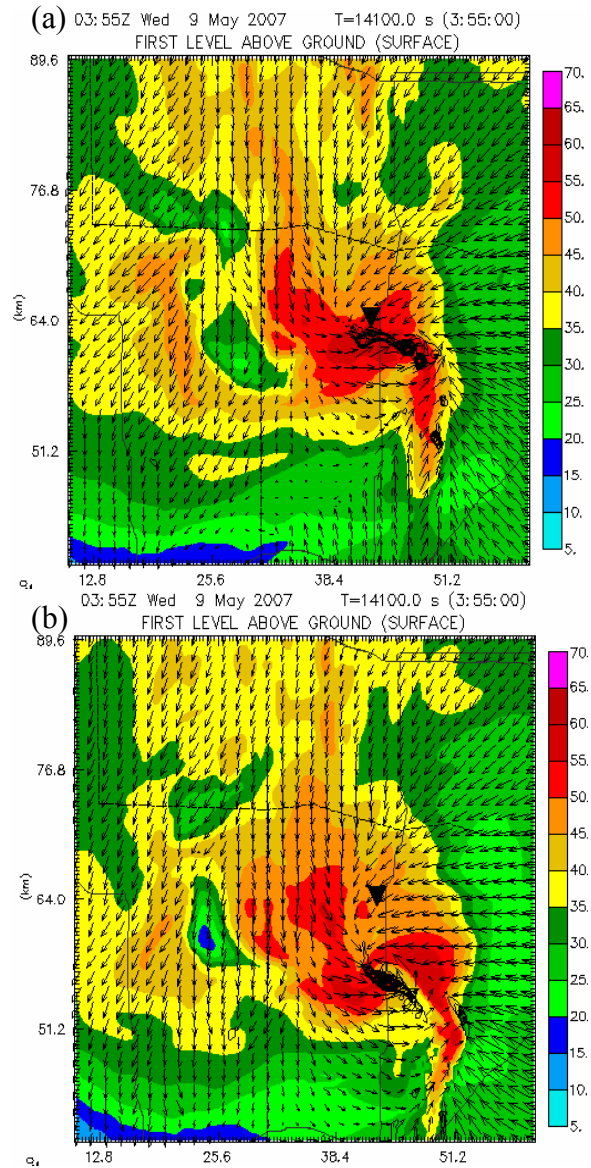


Fig. 9. Surface level forecast at 0355 UTC 9 May 2007 from (a) EXP8 and (b) EXP7. Reflectivity is shaded, contours are vorticity, and the black triangle indicates the reported tornado location.

establish what meteorological features are leading to a better forecast when CASA data are assimilated.

*Acknowledgements.* This work was supported primarily by the Engineering Research Centers Program of the National Science Foundation under NSF Cooperative Agreement No. EEC-0313747. Any Opinions, findings and conclusions or recommendations expressed in this material are those of the authors and do not necessarily reflect those of the National Science Foundation.

This project utilized high resolution surface data from the Oklahoma Mesonet provided by the Oklahoma Climatological Survey.

The computations for the data assimilation and forecasts were done on the facilities generously provided by the OU Supercomputing Center for Education and Research (OSKER). Thanks to Henry Neeman, OSKER Director, and Brandon George, OSKER system administrator, for their help.

## 6. REFERENCES

- Albers, S.C., J.A. McGinley, D.A. Birkenhuer, and J.R. Smart, 1996: The local analysis and Prediction System (LAPS): Analysis of clouds, precipitation and temperature. *Wea. and Forecasting*, **11**, 273-287.
- Brewster, K. A., 1996: Application of a Bratseth analysis system including Doppler radar. *Preprints, 15th Conference on Wea. Analysis and Forecasting*, Norfolk VA, Amer. Meteor. Soc., Boston, 92-95.
- Brewster, K.A., 2002: Recent advances in the diabatic initialization of a nonhydrostatic numerical model. *Preprints, 21st Conf. on Severe Local Storms, and Preprints, 15th Conf. Num. Wea. Pred. and 19th Conf. Wea. Anal. Forecasting*, San Antonio, TX, Amer. Meteor. Soc., J51-54.
- Brewster, K.A., L. White, B. Johnson, and J. Brotzge, 2005b: Selecting the sites for CASA NetRad, a collaborative radar network. *Ninth Symposium on Integrated Observing and Assimilation Systems for the Atmosphere, Oceans and Land Surface (IOAS-AOLS), 85th Amer. Meteor. Soc. Annual Meeting CD*, Paper: P3.4.
- Brewster, K. A., K. W. Thomas, J. Brotzge, Y. Wang, D. Weber, and M. Xue, 2007: High resolution data assimilation of CASA X-band radar data for thunderstorm forecasting. 22nd Conf. Wea. Anal. Forecasting/18th Conf. Num. Wea. Pred., Salt Lake City, Utah, Amer. Meteor. Soc., CDROM 1B.1.
- Brock, F. V., K.C. Crawford, R. L. Elliott, G. W. Cuperus, S. J. Stadler, H. L. Johnson, and M.D. Eilts, 1995: The Oklahoma Mesonet: a technical overview. *J. Atmos. Oceanic Technol.*, **12**, 5-19.
- Brotzge, J., K. Brewster, V. Chandrasekar, B. Philips, S. Hill, K. Hondl, B. Johnson, E. Lyons, D. McLaughlin, and D. Westbrook, 2007: CASA IP1: Network operations and initial data. Preprints, 23rd International Conf. on Interactive Information Processing Systems (IIPS) for Meteor., Ocean., and Hydrology, AMS Conf., San Antonio, TX.
- Gao, J.-D., M. Xue, K. Brewster, and K. K. Droegemeier, 2004: A three-dimensional variational data analysis method with recursive filter for Doppler radars. *J. Atmos. Ocean. Tech.*, **21**, 457-469.
- Hu, M., M. Xue, and K. Brewster, 2006a: 3DVAR and Cloud Analysis with WSR-88D Level-II Data for the Prediction of Fort Worth Tornadoic Thunderstorms Part I: Cloud analysis. *Mon. Wea. Rev.*, **134**, 675-698.
- Hu, M., M. Xue, J.-D. Gao and K. Brewster: 2006b: 3DVAR and Cloud Analysis with WSR-88D Level-II Data for the Prediction of Fort Worth Tornadoic Thunderstorms Part II: Impact of radial velocity analysis via 3DVAR, *Mon Wea Rev.*, **134**, 699-721.
- Hu, M. and M. Xue, 2007: Impact of configurations of rapid intermittent assimilation of WSR-88D radar data for the 8 May 2003 Oklahoma City tornadoic thunderstorm case. *Mon. Wea. Rev.*, **135**, 507-525
- Johnston, E.C., 1981: Mesoscale Vorticity Centers Induced by Mesoscale Convective Complexes. Master's Thesis, University of Wisconsin.
- Lin, Y.-L., R. D. Farley, and H. D. Orville, 1983: Bulk parameterization of the snow field in a cloud model. *J. Climate Appl. Meteor.*, **22**, 1065-1092.

McLaughlin, D.J., V. Chandrasekar, K. Droegemeier, S. Frasier, J. Kurose, F Junyent, B. Philips, S. Cruz-Pol, and J. Colom, 2005: Distributed Collaborative Adaptive Sensing (DCAS) for Improved Detection, Understanding, and Prediction of Atmospheric Hazards. 9th Symp. Integrated Obs. Assim. Systems - Atmos. Oceans, Land Surface (IOASAOLS), Amer. Meteor. Soc., San Diego, CA.

Menard, R. D., and J. M. Fritsch, 1989: A mesoscale convective complex-generated inertially stable warm core vortex. *Mon. Wea. Rev.*, **117**, 1237-1261.

Schaefer, J. T., 1990: The critical success index as an indicator of warning skill. *Wea. Forecasting*, **5**, 570-575.

Zhang, J., F. Carr and K. Brewster, 1998: ADAS cloud analysis. *Preprints, 12<sup>th</sup> Conf. on Num. Wea. Prediction*, Phoenix, AZ, Amer. Meteor. Soc., Boston, 185-188.